

# Predicting the temperature/pressure dependent density of biodieselfuels

**Nguyen Huynh Dong, Nguyen Thi Thuy**  
*Petrovietnam Manpower Training College*  
**Van Dinh Son Tho**  
*Hanoi University of Science and Technology*

## Abstract

*The purpose of this work was to develop a method for predicting temperature/pressure dependent density of biodiesel based on fatty acid ester composition. The PC-SAFT equation of state combined with a modified group contribution method was used to calculate density of mixtures of fatty acid esters. Prediction errors at atmospheric pressure were less than 0.5% for 10 multi-component mixtures of fatty acid ethylesters. Compared with experimentally measured density at 0.1 - 45MPa, the predicted densities of soybean, rapeseed, palm, mixture of soybean and rapeseed, mixture of palm and rapeseed, mixture of soybean and palm, mixture of soybean and rapeseed and palm, sunflower biodiesel were all within 1%.*

## Introduction

Biodiesel is a promising alternative energy resource for diesel fuel. Typically, biofuel consists of alkyl monoesters of fatty acids, obtained from vegetable oils or animal fats combined with a short-chain alcohol [1, 2]. Those esters have properties similar to ordinary diesel fuel made from crude oil and can be used in conventional diesel engines without any motorization transformation. Of the various alternate fuels under consideration, at this moment, biodiesel is the most promising alternative fuel to conventional diesel fuel (derived from fossil fuels; hereafter just "diesel") due to the following reasons [3, 4]:

- Biodiesel can be used in existing engines up to certain percentages (normally 20%) without any modification.
- Biodiesel is made entirely from vegetable sources. Therefore, biodiesel does not contain any sulfur, aromatic hydrocarbons, metals or crude oil residues.
- Biodiesel is an oxygenated fuel; emissions of carbon monoxide and soot tend to be reduced compared to conventional diesel fuel.
- Unlike fossil fuels, the use of biodiesel does not contribute to global warming as CO<sub>2</sub> emitted is once again absorbed by the plants grown for vegetable oil/biodiesel production. Thus CO<sub>2</sub> balance is maintained;

- The Occupational Safety and Health Administration classifies biodiesel as a non-flammable liquid (flash point of 160°C).

- The use of biodiesel can extend the life of diesel engines because it is more lubricating than petroleum diesel fuel.

- Biodiesel is produced from renewable vegetable oils/ animal fats and hence improves fuel or energy security and economic independence.

To optimize biodiesel manufacturing, many reported studies have built simulation models to quantify the relationship between operating conditions and process performance. For mass and energy balance simulations, it is essential to know the four fundamental thermophysical properties of the feed oil: liquid density ( $\rho^L$ ), vapor pressure ( $P^{vap}$ ), liquid heat capacity ( $C^L$ ), and heat of vaporization ( $\Delta H^{vap}$ ) [5 - 8].

Biodiesel fuel has to fulfil a number of quality standards. In Europe, the biodiesel fuel standards are compiled in the Norm CEN EN 14214 [9], in USA, in the ASTM D6751 [10] and in Vietnam in the TCVN 7717-07 [11]. Norms specify minimum requirements and test methods for biodiesel fuel to be used in diesel engines and for heating purposes, to increase the biodiesel fuel quality and its acceptance among consumers. Density is

an important fuel property because injection systems, pumps, and injectors must deliver an amount of fuel precisely adjusted to provide proper combustion [12]. As Tziourtzioumis and Stamatelos [13], Boudy and Seers [14] explained, from the evaluation of the effect of different fuel properties on the injection process of common rail direct-injection systems, density is the main property controlling the pressure wave in common rail systems and, subsequently, the total mass injected. Density data are required to be known to properly design reactors, distillation units and separation process, storage tanks, and process piping [15]. Knowledge and description of biodiesel densities as a function of the pressure and temperature are therefore required for a correct biodiesel formulation and a proper design and optimization of common rail engine injection systems for a precisely adjusted amount of fuel to be delivered to provide a proper combustion while minimizing  $\text{NO}_x$  emissions [16]. Knowledge of the density at varied temperature and pressure conditions is necessary in calculations of design equipment and to simulate the physico-chemical processes (they are involved in the equations of heat, mass, and momentum transfer). The density of liquids can be determined experimentally, but may be correlated and estimated by different analytical relations. These analytical expressions and models are usually based on adjustable parameters for each fluid and on the group contribution methods [17].

Rapeseed, soybean, and palm oils are the most commonly used oils to produce biodiesel although non-edible oils, such as *Jatropha*, are becoming more important [15]. The capacity to correctly predict biodiesel densities is of major relevance for a correct formulation of an adequate blend of raw materials aiming at producing biodiesel according to the required quality standards with the lowest production costs. Three main types of methods exist for estimating liquid densities of pure compounds. The first types are the methods based on the corresponding states theory, such as the Rackett equation and the Spencer and Danner method [15, 18 - 20]. These methods have, however, some disadvantages, such as the requirement of critical properties, and because they often use experimental-data-adjusted parameters, they have a limited predictive ability. The second type of method is based on mixing rules, such as Kay's [21] that allow for the estimation of a mixture density provided that the composition of the fuel and the densities of the pure compounds are known. They are only applicable to

simple mixtures with a near ideal behavior. Finally, group contribution models are another approach that only requires the chemical structure of the desired molecule to be known to estimate the thermophysical properties, such as liquid densities. The group contribution method GCVOL [22] is a predictive model that was able to provide pure fatty acid methyl ester (FAME) density descriptions within 1% deviation [23].

This article presents the results from a comprehensive evaluation of the methods for predicting liquid density of various biodiesel in function of temperature and/or pressure. The predictive capability of the modified GC-PC-SAFT model was tested against experimental data from 278 - 363K and 0.1 - 45MPa for 10 biodiesels.

### PC-SAFT Equation of state (PC-SAFT EoS)

The PC-SAFT EoS has a clear physical molecular model, which assumes that the molecule is composed of chains of freely jointed spherical segments. Several intermolecular forces are considered. They are divided into different contributions, correspondingly [24]. For non-associating compounds, it consists of an ideal gas contribution, a hard-chain contribution, and a perturbation contribution which accounts for the attractive interactions. The residual Helmholtz free energy is given in terms of a perturbation expansion:

$$a = a^{\text{id}} + a^{\text{hc}} + a^{\text{disp}} + a^{\text{dipole}} \quad (1)$$

More details of PC-SAFT EoS are described clearly in the original literature [24]. PC-SAFT is applied to mixtures using the van der Waals one-fluid model [24, 25] and modified Lorentz-Berthelot mixing rules that relate the potential parameters  $\varepsilon_{ij}$  and  $\sigma_{ij}$  for cross-interactions i-j to those of self-interactions i-i and j-j:

$$\varepsilon_{ij} = (1 - k_{ij}) \sqrt{\varepsilon_{ii} \varepsilon_{jj}} \quad (2)$$

$$\sigma_{ij} = (1 - l_{ij}) \left( \frac{\sigma_{ii} + \sigma_{jj}}{2} \right) \quad (3)$$

In many cases, pure prediction may be obtained by setting  $k_{ij} = l_{ij} = 0$  [26 -28]. In this study, we will therefore retain this hypothesis here as well.

### The dipole term

The  $a^{\text{dipole}}$  term refers to any contributions of the relevant contributions developed to account for polar interactions. Dipole-dipole is the most prominent electrostatic force in oxygenated compounds, such as

alkyl-esters. We consider only the dipole-dipole expressions from Gross and Vrabec (GV) [29] and from Jog and Chapman (JC) [30].

Jog and Chapman [30] developed a dipolar contribution by visualizing non-spherical polar molecules as hard-sphere chains containing both polar and non-polar segments. In this approach, the reference fluid is an equimolar mixture of non-polar and polar hard spheres, where the latter possesses a dipole vector at the center of the sphere. The thermodynamic properties of the polar hard spheres were calculated using the u-expansion [31]. Jog and Chapman showed, using computer simulation, that  $g^R$  can be approximated by the hard-sphere rdf,  $g^{hs}$ , up to a moderate dipole strength provided that the segment dipole vector is aligned perpendicularly to the line joining the center of the dipole segment to that of the adjacent segment. The dipolar term was presented as a perturbation expansion in Padé approximant (JC approach) [32]:

$$a = a_0 + a_2 \left[ \frac{1}{1 - \frac{a_3}{a_2}} \right] \quad (4)$$

$$a_2^{dipole} = -\frac{2\pi N\rho}{3kT} \sum_{\alpha\beta} x_\alpha x_\beta x_{p\alpha}^\mu x_{p\beta}^\mu m_\alpha m_\beta \frac{\mu_\alpha^2 \mu_\beta^2}{d_{\alpha\beta}^3} J_{\alpha\beta}^{(6)} \quad (5)$$

$$a_3^{dipole} = \frac{32}{135} \left( \frac{14\pi}{5} \right)^{1/2} \frac{N\rho^2}{(kT)^2} \sum_{\alpha\beta\gamma} x_\alpha x_\beta x_\gamma x_{p\alpha}^\mu x_{p\beta}^\mu x_{p\gamma}^\mu m_\alpha m_\beta m_\gamma \frac{\mu_\alpha^2 \mu_\beta^2 \mu_\gamma^2}{(d_{\alpha\beta} d_{\alpha\gamma} d_{\beta\gamma})} K_{\alpha\beta\gamma} (222;333) \quad (6)$$

Where  $m$  stands for chain parameter;  $\rho$  is the number density of molecules;  $k$  is the Boltzmann constant;  $T$  is the temperature;  $d_{\alpha\beta}$  is the average diameter of segment  $\alpha$  and  $\beta$ ,  $\mu_\alpha$  are the dipole moment of component  $\alpha$ .  $x_{p\alpha}$  refer to the fraction of polar segment in  $\alpha$  chain of component  $\alpha$ , whereas  $x_\alpha$  is the mole fraction of component  $\alpha$ .  $J$  and  $K$  are the angular pair and triplet correlation. These integrals are a function of reduced density and temperature and have the empirical form as described in [33].

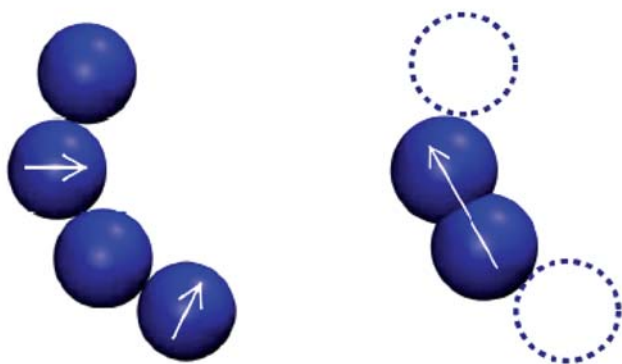


**Fig.1.** Orientation of the dipole moment within a chain molecule, following the JC (left) or the GV (right) approach. In the JC approach, the dipole vectors, shown as white arrows, are placed on specific segments within a chain, perpendicular to the vector connecting the centers of adjacent segments. In the GV approach, the dipole moment is stretched across a maximum of two segments, and placed along the central axis. Its position, with respect to the other non-polar segments, is irrelevant

The notion of  $x_p$  as an adjustable parameter is, however, not entirely correct. Various authors [34, 35] chose to correlate  $x_p$  by assigning a constant value to the product  $m \cdot x_p$  for a particular homologous group. To determine this constant, the smallest member of the series is fitted to vapour pressure and liquid density data, with no constraints on  $x_p$ . The product  $m \cdot x_p$  stemming from the final set of parameters is then held constant for the rest of the homologous group. Different authors [32, 36] observed the problem of multiple solutions when fitting a set of  $\epsilon/k$ ,  $\sigma$ ,  $m$  parameters, and suggested the incorporation of a single set of binary data in the regression. Any mixture with a second component free of functionality (e.g. n-alkanes) could be used.

Such segment approach of the JC term differs from that of the GV term in that the dipolar moment is not placed along the molecular axis of the molecule. In the GV approach, the location of the stretchable dipole in the chain is not considered. This is depicted graphically in Fig. 1. The dipole segments exist site-like in a JC chain; thus the distance of closest approach of the dipole is represented. Furthermore, the segment approach also accounts for multiple dipolar functional groups. Al-Saifi et al. [37] compared the Helmholtz free energy contribution to the reduced chemical potential from the two dipolar terms, and found the JC approach to have a higher contribution among the two.

### Modeling esters using a modified group contribution method

Such a thermodynamic treatment of esters requires first a definition of the chemical groups found in an ester molecule. Let us recall that the general chemical formulas of esters  $RCOOR'$

where  $R$  and  $R'$  are hydrocarbon chains. In this work, we have considered only the case when  $R$  and  $R'$  were linear alkyl chains. This means that  $R$  and  $R'$  may be explicitly written as  $\text{CH}_3-(\text{CH}_2)_n$  and  $\text{CH}_3-(\text{CH}_2)_{n'}$  with  $n, n' \geq 0$ . Therefore, three different chemical groups are used in this work:  $\text{CH}_3$ ,  $\text{CH}_2$ , and  $\text{COO}$ .

In the spirit of the GC method mentioned above, the EoS parameters of a given ester  $\text{RCOOR}'$  are computed by the following relations [38]:

$$\varepsilon = n^T \sqrt{(\varepsilon_{\text{CH}_2})^{n_{\text{CH}_2}} \cdot (\varepsilon_{\text{CH}_3})^{n_{\text{CH}_3}} \cdot (\varepsilon_{\text{COO}})^{n_{\text{COO}}}} \quad (7)$$

$$\sigma = \frac{\sigma_{\text{CH}_2} \cdot n_{\text{CH}_2} + \sigma_{\text{CH}_3} \cdot n_{\text{CH}_3} + \sigma_{\text{COO}} \cdot n_{\text{COO}}}{n^T} \quad (8)$$

Where  $n_{\text{CH}_2}$ ,  $n_{\text{CH}_3}$  and  $n_{\text{COO}}$  are respectively the numbers of groups  $\text{CH}_2$ ,  $\text{CH}_3$ , and  $\text{COO}$  in the ester molecule and  $n^T = n_{\text{CH}_2} + n_{\text{CH}_3} + n_{\text{COO}}$  is the total number of groups in the molecule. The chain parameter  $m$  may be correlated through a simple linear correlation to the different group numbers, involving a chain contribution parameter denoted  $R_i$  for each group  $i$ .

$$m = S_{\text{CH}_2} R_{\text{CH}_2} \cdot n_{\text{CH}_2} + S_{\text{CH}_3} R_{\text{CH}_3} \cdot n_{\text{CH}_3} + S_{\text{COO}} R_{\text{COO}} \cdot n_{\text{COO}} \quad (9)$$

$S_{\text{CH}_2}$ ,  $S_{\text{CH}_3}$ ,  $S_{\text{COO}}$  are "shape factor" which corresponds to the proportion of the spherical united-atom group that contributes to the properties of the molecule, in this work,  $S_{\text{CH}_3}$ ,  $S_{\text{COO}}$  are unity and  $S_{\text{CH}_2}$  were reused from a previous paper [39].

As suggested by a similar approach [40] proposed to model and to make a distinction between two oxygenated isomers using the chain lengths  $m$  of the two molecules,  $R_{\text{COO}}$  is regarded as a function of the  $\text{COO}$  group position  $p$  in the ester chain, defined by  $p = \min(n_R, n_{R'}) + 1$  [40]. The dipole moment was supposed to follow an empirical linear relation with  $n_R - n_{R'}$  that is written for  $\text{RCOOR}'$  as:

Where  $\mu_0$ ,  $\mu_1$ , and  $\mu_2$  are adjustable parameters [40].

$$\mu = \mu_0 - \mu_1 \left(1 - \frac{1}{n_R}\right) - \mu_2 \left(1 - \frac{1}{n_{R'}}\right) \quad (10)$$

### Parameterization of the PC-SAFT

Depending on the form of the PC-SAFT employed, different numbers of pure component parameters must be determined for the model. To reflect real substance behaviour, the parameters are regressed to experimental data of thermodynamic properties. For non-associating substances, the chain segment  $m$ ; the segment diameter  $\sigma$ ; and the depth of energy well  $\varepsilon/k$  are always included

in the regression. The parameters  $m$  and  $\sigma$  are geometric parameters and reflect the packing extent of the molecule. Data on liquid density ( $\rho^l$ ) supply information on the magnitude of these two parameters.  $\varepsilon/k$  is an attractive energetic parameter that holds molecules together. Its magnitude affects the molecules' tendency to disperse and form a vapour phase. Values of the vapour pressure ( $P^{\text{sat}}$ ) are required to tune the parameter.

As with multi-parameter EoS, the parameterization of PC-SAFT is subjected to the modeler's preferences. The central theme of this work is the application of PC-SAFT to the calculation of thermodynamic properties. Therefore we devise herein a systematic procedure for tuning the model for phase equilibria purposes. The procedure outlined below can be easily modified to yield different sets of parameters adapted for alternative purposes:

- Visualize the compound. This helps identify whether the compound is associating/non-associating, polar/non-polar, and define chemical group structure;
- Compile data. As explained, experimental data on liquid densities and vapour pressures are essential, and as many data as possible should be collected from the triple point to the critical point. This ensures the parameters are applicable for the entire range of vapour-liquid coexistence.
- Eliminate unwanted data. It is useful to obtain empirical correlations for the liquid volumes and vapour pressures. A plot of the collected data and an empirical correlation on the same axes may reveal significant outliers that would otherwise mislead the regression if retained. These outliers should be removed.
- Parameter regression. Using logical initial guesses to regress the relevant parameters so as to minimize the objective function  $F$ :

$$F = 100 \sum_{Tp} \frac{1}{N_{\text{exp}, Tp}} \sum_i^{N_{\text{exp}, Tp}} \left( \frac{\theta_{Tp,i}^{\text{exp}} - \theta_{Tp,i}^{\text{cal}}}{\theta_{Tp,i}^{\text{exp}}} \right)^2 \quad (11)$$

Where  $T_p$  is the thermodynamic property to be fitted;  $NT_p$  is the total number of different types of thermodynamic properties to be considered in the overall regression;  $N_{\text{exp}, Tp}$  is the total number of experimental datapoints considered for thermodynamic property  $T_p$ ; and  $\theta_{Tp,i}^{\text{exp/cal}}$  is the  $i^{\text{th}}$  experimental/calculated value of the thermodynamic property  $T_p$ . Only discrete experimental data are used in the regression.

- Evaluate the results. The absolute average deviation, AAD (in % unit), is calculated as following:

$$AAD_{Tp} = \frac{100}{N_{exp,Tp}} \sum_i^{N_{exp,Tp}} \left( \frac{\theta_{Tp,i}^{exp} - \theta_{Tp,i}^{cal}}{\theta_{Tp,i}^{exp}} \right) \quad (12)$$

PC-SAFT is not sufficiently high for such purpose, and over-expansion of objective function only serves to complicate the optimization routine. However, the predictions of the heat capacity (Cp) and the speed of sound (w) for some non-associating and associating compounds, whose parameters were regressed to liquid densities and vapour pressures. Even though Cp and w were not included in the regression of pure-component parameters, qualitative agreements with experimental data could still be achieved. This emphasizes the appropriateness of the choice of  $\rho^L$  and  $P^{sat}$  as target properties, as well as the physical basis of the model.

**Parameters for Fatty acid methyl esters**

Fatty acid methyl esters (FAME) of high molecular weights are the main products of the transesterification of triglycerides to form biodiesel components [41]. Accurate determination of thermodynamic properties such as vapour pressure (normal boiling point), density, viscosity and latent heat of vaporization are important to ensure

good fuel quality control. Nguyen Thi et al. [42] used a group-contribution SAFT (GC-SAFT) approach to model heavy esters from methyl propanoate to eicosanoate using three different versions of SAFT and the Kraska and Gubbins dipolar term. Nguyen Huynh et al. [40] later extended this work to mixtures of heavy esters, using the Jog and Chapman dipolar term. Tihic et al. [43] applied the group-contribution simplified PC-SAFT (sGCPC-SAFT) to the prediction of vapour pressures of heavy esters, and presented calculations on phase equilibria and infinite dilution activity coefficients. Pratas et al. [44] used CPA EoS to predict the high-pressure density data of pure FAMES and biodiesels. As far as the Perturbed-Chain form of the SAFT EoS is concerned, the various sources proceeded to present similar errors in predicting vapour pressures, ranging from 1% to as high as 40% deviations. While the different approaches adopted by the above sources make them not strictly comparable, most highlighted the importance of experimental data to improve the predictability of their models.

The objective in this work is to present parameters (predict) for FAME from methyl caprate ( $C_{11}H_{22}O_2$ ) to methylignocerate ( $C_{25}H_{50}O_2$ ), which could be used with the PC-SAFT EoS. There is a striking lack of thermodynamic data

**Table 1.** Relative deviations on vapor pressures and saturated liquid volumes of the regression database compounds (accepted data in DIPPR[50])

Compounds	Formular	Npt.	T <sub>rang</sub> (K)	AAD P <sup>sat</sup> (%)	Npt.	T <sub>rang</sub> (K)	AAD $\rho^{liq}$ (%)
Alkyl acetate (CCOOR')							
Ethyl acetate	CCOOC <sub>2</sub>	16	233 - 522	2.79	13	273 - 503	5.89
Propyl acetate	CCOOC <sub>3</sub>	14	273 - 543	3.38	14	273 - 533	2.91
Butyl acetate	CCOOC <sub>4</sub>	8	326 - 410	2.96	12	273 - 393	0.25
Pentyl acetate	CCOOC <sub>5</sub>	12	281 - 599	4.40	12	273 - 417	0.71
Hexyl acetate	CCOOC <sub>6</sub>	7	304 - 441	2.33	10	273 - 363	1.01
Heptyl acetate	CCOOC <sub>7</sub>	10	349-462	3.41	5	273 - 303	1.06
Octyl acetate	CCOOC <sub>8</sub>	8	334 - 484	6.39	7	293 - 368	1.22
Nonyl acetate	CCOOC <sub>9</sub>	11	293 - 661	16.95	2	288 - 298	1.02
Decyl acetate	CCOOC <sub>10</sub>	9	348 - 518	11.18	6	293 - 368	1.04
Methyl ester (RCOOC)							
Methyl propanoate	C <sub>2</sub> COOC	29	253 - 530	1.13			
Methyl butanoate	C <sub>3</sub> COOC	10	293 - 313	2.72			-
Methyl pentanoate	C <sub>4</sub> COOC	7	293 - 328	3.17			-
Methyl hexanoate	C <sub>5</sub> COOC	8	297 - 333	5.05			-
Methyl heptanoate	C <sub>6</sub> COOC	8	310 - 340	1.29			-
Methyl octanoate	C <sub>7</sub> COOC	7	312 - 348	5.85			-
Methyl nonanoate	C <sub>8</sub> COOC	10	308 - 353	3.45			-
Methyl decanoate	C <sub>9</sub> COOC	11	310 - 351	4.89			-
Methyl Undecanoate	C <sub>10</sub> COOC	7	331 - 351	1.13			-

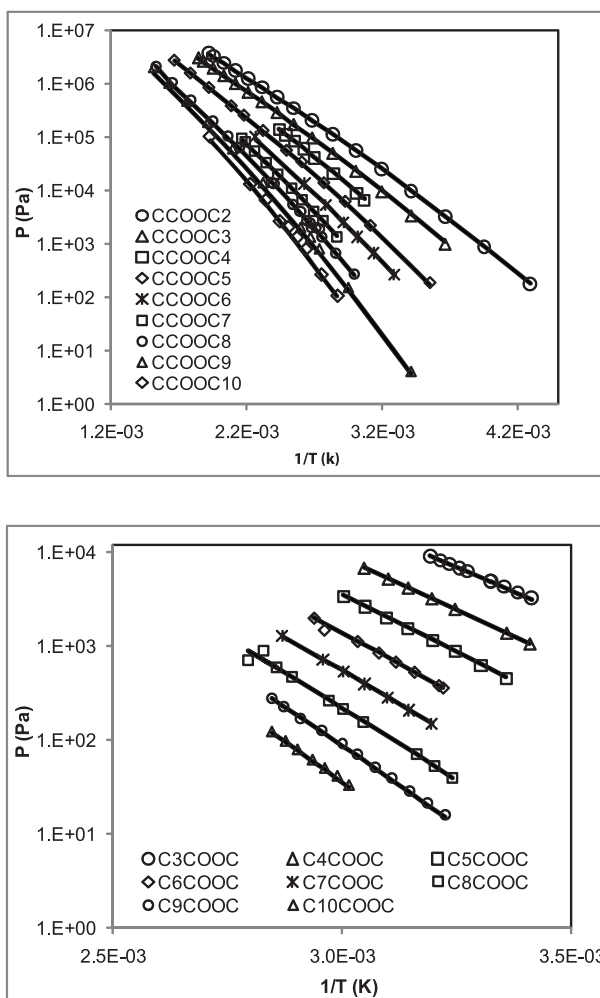


**Fig. 2.** Vapor pressure of the FAME ester. The symbols represent the experimental data [50], while the continuous curves correspond to the mGC-PC-SAFT description with the parameters estimated in this work

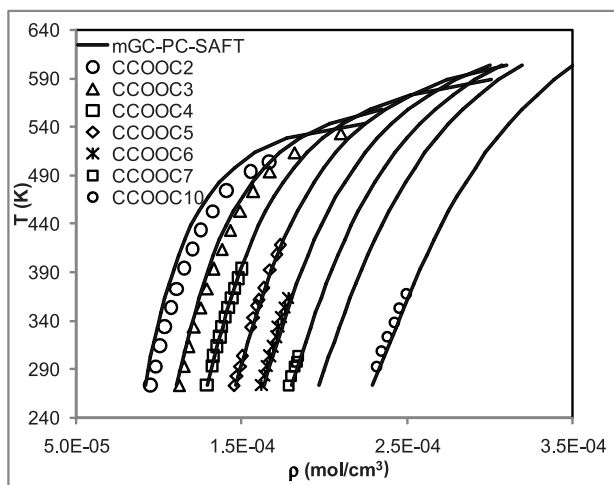


**Fig. 3.** Saturated liquid densities of the FAME esters. The symbols represent the experimental data [50], while the continuous curves correspond to the mGC-PC-SAFT description with the parameters estimated in this work

for FAME (an overview can be found at <http://www.ddbst.com/files/ddbsp/DDBSP-Biodiesel-2006.pdf>) and most of the better quality data on FAME vapour pressures are believed to be from Scott et al. [45], Rose and Supina [46], and van Genderen et al. [47]. The number of data points decrease with the increasing number of carbon atoms, due to difficulties in precise measurements of increasingly low pressures (e.g. the vapour pressure of methyl stearate at 316K is 9.96mPa [47]). Liquid density data can be found in the work of Pratas et al. [23, 48, 49].

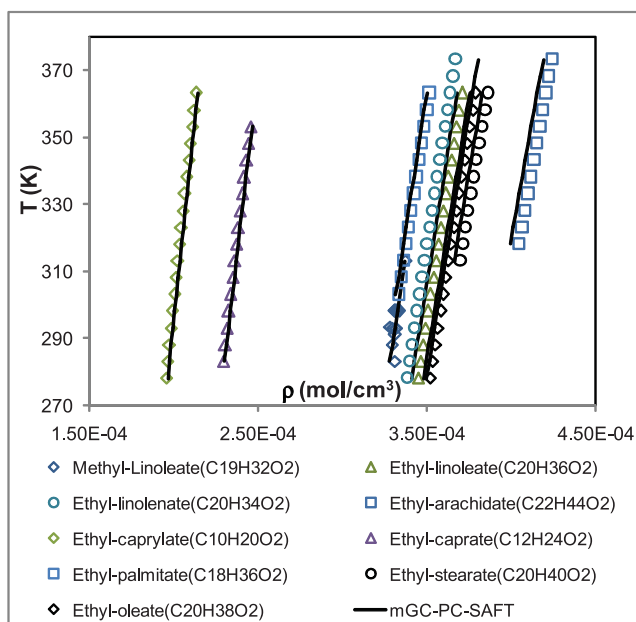
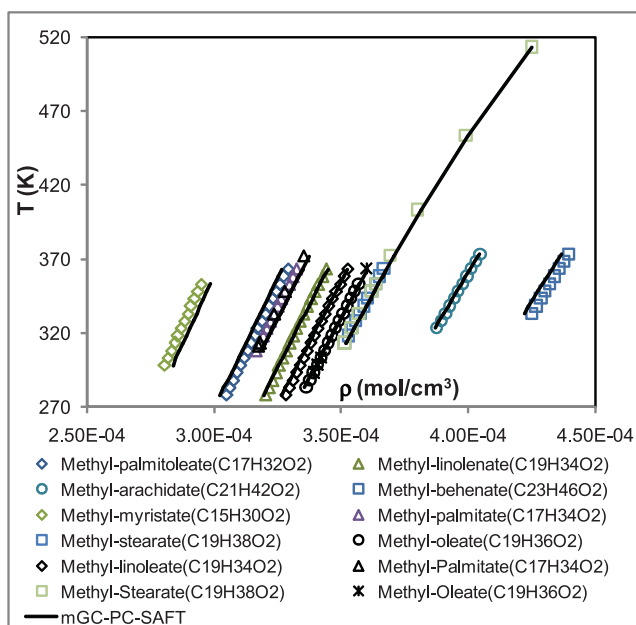


**Fig. 4.** Prediction of liquid density of alkyl esters series. The symbols represent the experimental data [23, 50], while the continuous curves correspond to the mGC-PC-SAFT prediction

**Table 2.** Prediction results of liquid density of some heavy esters. Experimental data are taken from [23, 50]

Compounds	T <sub>rang</sub> (K)	ρ <sub>min</sub> (mol/cm <sup>3</sup> )	ρ <sub>max</sub> (mol/cm <sup>3</sup> )	AAD (%)	Npt
Methyl-caprylate (C <sub>9</sub> H <sub>18</sub> O <sub>2</sub> )	283 - 353	1.79E-04	1.92E-04	2.20	15
Ethyl-caprylate (C <sub>10</sub> H <sub>20</sub> O <sub>2</sub> )	278 - 363	1.96E-04	2.14E-04	0.58	18
Methyl-caprate (C <sub>11</sub> H <sub>22</sub> O <sub>2</sub> )	278 - 363	2.11E-04	2.29E-04	1.93	18
Ethyl-caprate (C <sub>12</sub> H <sub>24</sub> O <sub>2</sub> )	283 - 353	2.30E-04	2.46E-04	0.42	15
Methyl-laurate (C <sub>13</sub> H <sub>26</sub> O <sub>2</sub> )	283 - 353	2.44E-04	2.61E-04	1.59	15
Methyl-myristate (C <sub>15</sub> H <sub>30</sub> O <sub>2</sub> )	298 - 353	2.81E-04	2.95E-04	1.17	12
Methyl-palmitoleate (C <sub>17</sub> H <sub>32</sub> O <sub>2</sub> )	278 - 363	3.05E-04	3.29E-04	0.67	18
Methyl-palmitate (C <sub>17</sub> H <sub>34</sub> O <sub>2</sub> )	308 - 363	3.17E-04	3.32E-04	0.71	12
Ethyl-palmitate (C <sub>18</sub> H <sub>36</sub> O <sub>2</sub> )	303 - 363	3.34E-04	3.52E-04	0.51	13
Methyl-linolenate (C <sub>19</sub> H <sub>34</sub> O <sub>2</sub> )	278 - 363	3.20E-04	3.44E-04	0.12	18
Methyl-linoleate (C <sub>19</sub> H <sub>34</sub> O <sub>2</sub> )	283 - 313	3.31E-04	3.38E-04	0.37	13
Methyl-oleate (C <sub>19</sub> H <sub>36</sub> O <sub>2</sub> )	283 - 353	3.36E-04	3.57E-04	0.10	15
Methyl stearate (C <sub>19</sub> H <sub>38</sub> O <sub>2</sub> )	313 - 513	3.51E-04	4.25E-04	0.24	10
Ethyl-linolenate (C <sub>20</sub> H <sub>34</sub> O <sub>2</sub> )	278 - 373	3.39E-04	3.67E-04	3.50	20
Ethyl-linoleate (C <sub>20</sub> H <sub>36</sub> O <sub>2</sub> )	278 - 363	3.45E-04	3.71E-04	0.91	18
Ethyl-stearate (C <sub>20</sub> H <sub>40</sub> O <sub>2</sub> )	313 - 363	3.70E-04	3.86E-04	0.90	11
Methyl-arachidate (C <sub>21</sub> H <sub>42</sub> O <sub>2</sub> )	323 - 373	3.88E-04	4.05E-04	0.18	11
Ethyl-arachidate (C <sub>22</sub> H <sub>44</sub> O <sub>2</sub> )	318 - 373	4.05E-04	4.24E-04	1.26	12
Methyl-erucate (C <sub>23</sub> H <sub>44</sub> O <sub>2</sub> )	278 - 363	4.00E-04	4.29E-04	0.85	18
Methyl-behenate (C <sub>23</sub> H <sub>46</sub> O <sub>2</sub> )	333 - 373	4.25E-04	4.39E-04	0.68	9
Methyl-lignocerate (C <sub>25</sub> H <sub>50</sub> O <sub>2</sub> )	338 - 373	4.61E-04	4.74E-04	1.20	8

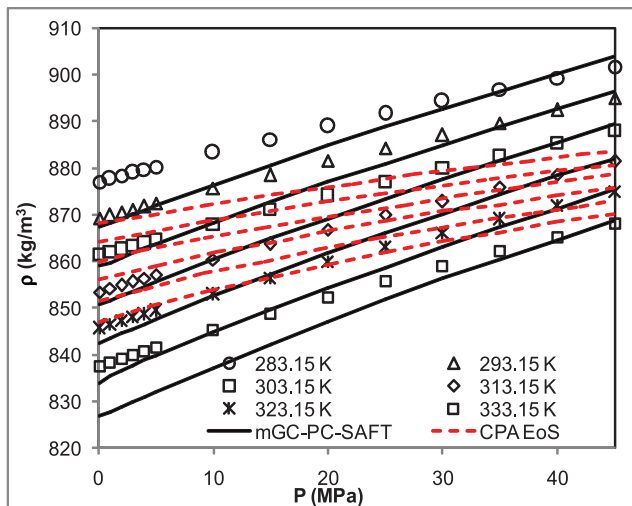


**Fig. 5.** Density isotherms for methyl laurate. Comparison between two models, (—) predicted by mGC-PC-SAFT (this work); (- - -) computed with CPA EoS [44]. Data taken from ref [44]

The relative deviations obtained on the vapor pressures and saturated liquid phase volumes for pure FAME are presented in Table 1. The T-P and T-ρ diagrams are given in Fig. 2. From this table, it appears that the mGC-PC-SAFT provide generally reasonable and comparable

correlations of pure esters VLE. The agreement between experimental and calculated vapor pressure is generally lower than 5% i.e. slightly better than the one obtained in previous work [40, 42].

### PpT predictions results for pure heavy esters

PpT calculations of heavier compounds using the modified group contribution PC-SAFT without adjustment on experimental data is a pertinent test of the predictive character of the approach. The results obtained on several representative compounds are displayed in Figs. 4 - 5 and Table 2 along with those obtained by other methods for comparison.

For the prediction, very good agreements can be seen between the model and the experimental data for esters up to ethyl-arachidate (< 2%). The predictions are poorer for Ethyl-linolenate (C<sub>20</sub>H<sub>34</sub>O<sub>2</sub>) (3.5%), but in fact they are quite reasonable if compared to those given by other predictive methods [40].

The comparison with other methods is not very easy since the different authors use different strategies

**Table 3.** Compositions of the Biodiesels Studied, in mass percentage. (S: soybean biodiesel, R: rapeseed biodiesel, P: palm biodiesel, SR: soybean + rapeseed biodiesel, PR: palm + rapeseed biodiesel, SP: soybean + palm biodiesel, SRP: soybean + rapeseed + palm biodiesel, Sf: sunflower biodiesel, GP and SoyA: soybean + rapeseed biodiesel)

Methyl-esters	Chemical formular	S	R	P	SR	PR	SP	SRP	Sf	GP	SoyA
C <sub>10</sub>	C <sub>11</sub> H <sub>22</sub> O <sub>2</sub>		0.01	0.03		0.02	0.01	0.01			
C <sub>12</sub>	C <sub>13</sub> H <sub>26</sub> O <sub>2</sub>		0.04	0.24	0.03	0.2	0.18	0.14	0.02	0.02	
C <sub>14</sub>	C <sub>15</sub> H <sub>30</sub> O <sub>2</sub>	0.07	0.07	0.57	0.09	0.54	0.01	0.38	0.07	0.13	
C <sub>16</sub>	C <sub>17</sub> H <sub>34</sub> O <sub>2</sub>	10.76	5.22	42.45	8.9	23.09	25.56	18.97	6.4	10.57	17.04
C <sub>16:1</sub>	C <sub>17</sub> H <sub>32</sub> O <sub>2</sub>	0.07	0.2	0.13	0.15	0.17	0.11	0.14	0.09	0.13	
C <sub>18</sub>	C <sub>19</sub> H <sub>38</sub> O <sub>2</sub>	3.94	1.62	4.02	2.76	3.02	4.04	3.28	4.22	2.66	3.73
C <sub>18:1</sub>	C <sub>19</sub> H <sub>36</sub> O <sub>2</sub>	22.96	62.11	41.92	41.82	52.92	33.13	42.51	23.9	41.05	28.63
C <sub>18:2</sub>	C <sub>19</sub> H <sub>34</sub> O <sub>2</sub>	53.53	21.07	9.8	37.51	15.47	31.72	27.93	64.16	36.67	50.45
C <sub>18:3</sub>	C <sub>19</sub> H <sub>32</sub> O <sub>2</sub>	7.02	6.95	0.09	7.02	3.08	3.58	4.66	0.12	7.1	
C <sub>20</sub>	C <sub>21</sub> H <sub>42</sub> O <sub>2</sub>	0.38	0.6	0.36	0.46	0.49	0.39	0.45	0.03	0.44	
C <sub>20:1</sub>	C <sub>21</sub> H <sub>40</sub> O <sub>2</sub>	0.23	1.35	0.15	0.68	0.67	0.2	0.52	0.15	0.67	
C <sub>22</sub>	C <sub>22</sub> H <sub>44</sub> O <sub>2</sub>	0.8	0.35	0.09	0.46	0.24	0.32	0.33	0.76	0.45	
C <sub>22:1</sub>	C <sub>22</sub> H <sub>42</sub> O <sub>2</sub>	0.24	0.19	0	0.12	0.09	0.12	0.14	0.08	0.12	
C <sub>24</sub>	C <sub>24</sub> H <sub>48</sub> O <sub>2</sub>		0.22	0.15			0.63	0.53			
Total		100	100	100	100	100	100	100	100	100	100

**Table 4.** Absolute Average Deviation between the measured density of biodiesel mixtures over the Temperature Range (278.15 to 363.15) K and those estimated by GCVOL Extension to High Pressures Models and comparing with the predicted results obtained by mGC-PC-SAFT. Experimental data are taken from ref. [49, 52 - 54]

Biodiesel mixture	T (K)	$\rho$ (kg/ m <sup>3</sup> )	GCVOL	mGC-PC-SAFT
S	278 - 363	832 - 894	0.52	0.23
R	278 - 363	831 - 893	0.74	0.43
P	278 - 363	823 - 893	0.47	0.53
SR	278 - 363	831 - 890	0.40	0.23
RP	278 - 363	827 - 890	0.30	0.50
SP	278 - 363	827 - 895	0.29	0.30
SRP	278 - 363	828 - 892	0.32	0.32
Sf	283 - 363	832 - 888	0.23	0.20
GP	283 - 363	830 - 888	-	0.11
SoyA	283 - 353	837 - 885	-	0.20

for group parameters regression on more or less wide compounds databases with or without mixtures and for different target systems, or apply their methods to compounds other than those investigated here, or give average deviations for data sets and data ranges different from those used in this study, or do not always give details on the database so true prediction cannot be distinguished from correlation.

As a matter of fact, the mGC-PC-SAFT deviations increase slightly with chain length but so do the deviations of the usual method which represent the best fit to the data with the given equation. It may be amazing

that in some cases, group contribution may give better liquid volume results than the direct fit of data [38]. But if one is reminded that both pressures and volumes are used for the fit, there is no contradiction, since the GC pressure deviations are greater and so are the overall deviations.

At least in the case of the work of Pratas et al. [44] was possible to give deviations for the liquid density on the same temperature and pressure ranges as a basis

for comparison on methyl-laurate, methyl-oleate and methyl-myristate (Fig. 5) and Table 5, mGC-PC-SAFT gives slightly better prediction than CPA EoS. The deviations may however appear slightly larger in the low pressure region, but in fact they are quite reasonable (maximum relative derivation is 1.94%) if compared to those given by other predictive methods [23, 51].

### Biodiesel fuels P $\rho$ T Prediction results and discussion

Here, pure predictions of liquid density of biodiesel (multi-component mixture) were made, which means that no binary interaction parameters were used

**Table 5.** Absolute Average Deviation for Biodiesel and Methyl Ester Densities at High Pressures Calculated with the CPA EoS and predicted with mGC-PC-SAFT. Experimental data are taken from ref. [44]

Component/ Biodiesel mixture	AAD %		
	CPA EoS		mGC-PC-SAFT
	$\rho(0.1 - 45 \text{ MPa})^*$	$\rho(0.1 - 45 \text{ MPa})^{**}$	$\rho(0.1 - 45 \text{ MPa})^{***}$
methyl-laurate	4.47	0.59	0.68
methyl-myristate	5.86	0.99	0.32
methyl-oleate	3.24	0.84	1.25
biodiesel S	-	0.79	0.43
biodiesel R	-	2.51	0.78
biodiesel P	-	1.13	0.50
biodiesel RP	-	1.07	0.43
biodiesel SR	-	0.82	0.42
biodiesel SP	-	1.25	0.43
biodiesel SRP	-	0.89	0.44

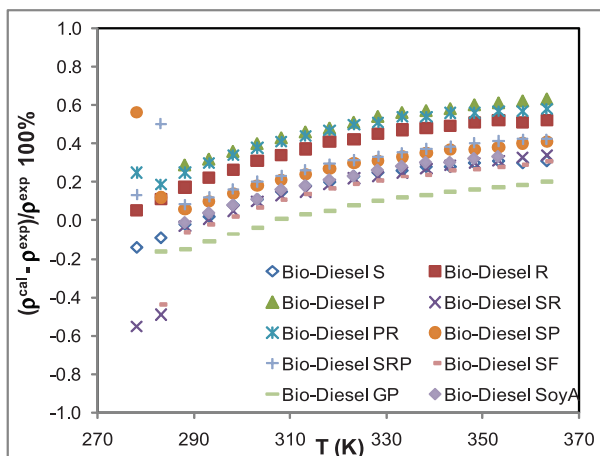
( $k_{ij} = l_{ij} = 0$ ). Various classes of biodiesel were investigated to test the validity of mGC-PC-SAFT applied to esters mixtures.

Table 3 reports methyl ester compositions for the biodiesels selected for this work. This information is of major importance because the fatty acid ester profiles of biodiesels determine their chemical and physical properties, such as densities [49].

To study the predictive ability of the mGC-PC-SAFT,

the AAD for the predicted densities for each biodiesel were estimated according to equation 12. The AAD for each biodiesel studied are reported in Table 4 and 5, while the AAD of the individual data points for the 10 biodiesel samples are shown in Fig.7.

Detailed prediction results of 10 bio-diesel mixtures at atmospheric pressure are reported in Table 4 and prediction results of liquid density for 3 pure heavy methyl-esters and 7 bio-diesel mixtures at 0.1 - 45MPa are grouped in Table 5. Very good predictions were obtained with mGC-PC-SAFT, with an AAD of about 0.50%, except in the case of methyl-oleate, unsaturated alkyl-ester. No significant differences between the results obtained with the GCVOL and mGC-PC-SAFT are observed (Table 4),



**Fig.7.** Absolute average deviation between experimental and predicted densities as a function of the temperature using mGC-PC-SAFT

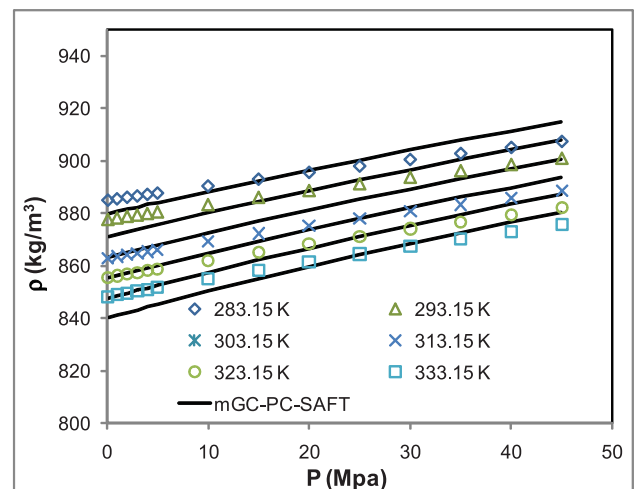
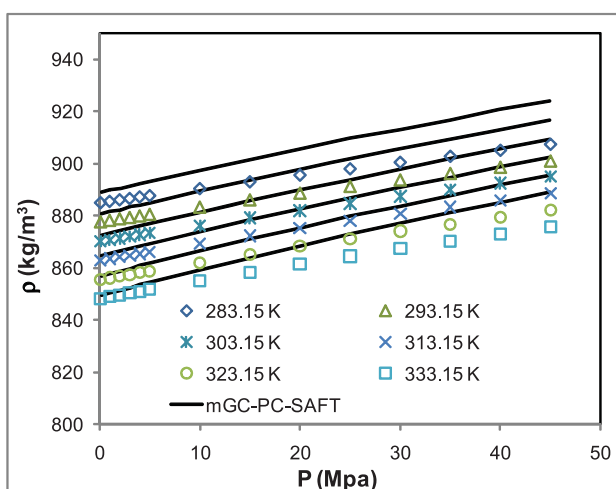


**Fig.8.** Density isotherms for rapeseed biodiesel (left) and palm biodiesel (right). The symbols represent the experimental data, while the continuous curves correspond to the mGC-PC-SAFT prediction

(\*) with FAME CPA pure compound parameters from correlations; (\*\*) with FAME CPA pure compound parameters correlated from pure component data. (\*\*\*) pure prediction results.

which may come as a surprise but can easily be justified by the similarity of the compounds in nature and size present in the biodiesels, resulting in similar concentration values regardless of the units adopted, resulting in a marginal

impact on the prediction (Fig.7).

The AAD for each biodiesel studied are reported in Table 4, while the relative deviation of the individual data points for the 10 biodiesel samples are shown on Fig.7.

Results from Pratas et al. [44] used CPA EoS to compute liquid density of biodiesel at high pressure showed in Fig.9 indicate that CPA EoS has a poorer performance for heavy ester and biodiesels at high pressure and high temperature, such as soybean biodiesel (Fig.9).

In most cases (Figs.8 - 11), mGC-PC-SAFT tends to over-predict mixture's density values at higher pressures (approach to the critical zone) and under-predict at low pressure region, this was the conclusion in very recent work by Burgess et al. [55] for PC-SAFT equation of state. Moreover, the pure-component mGC-PC-SAFT parameters of heavy compounds are predicted using the equations 7 - 10, belong to their chemical structure, that might effect the model's accuracy (the derivations are however smaller than 1%, Fig. 7). Although a correction term can be applied

to the  $\epsilon/k$  parameter to make high pressure high temperature (HTHP) PC-SAFT pure-component density predictions, only slightly inferior to predictions with the original PC-SAFT parameters, but vapor-liquid equilibrium predictions with the original PC-SAFT parameters are clearly superior to predictions made with the HTHP parameters [55].

It was shown that representation of mixtures  $P_{Txy}$  and  $\rho_{PT}$  can be improved if the binary interaction parameters are taken into account [35, 56], for the sake of simplicity, all zero binary interaction parameters were assumed here, but remain acceptable results.

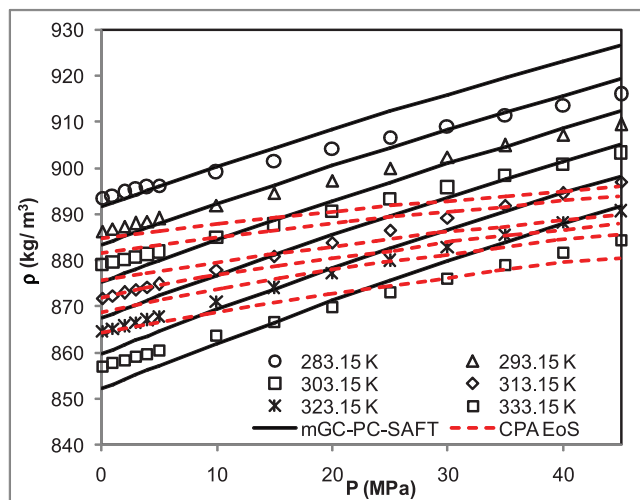


**Fig.9.** Density isotherms for soybean biodiesel. Comparison between two models, (—) predicted by mGC-PC-SAFT; (---) computed with CPA EoS [44]. Data taken from ref. [44]

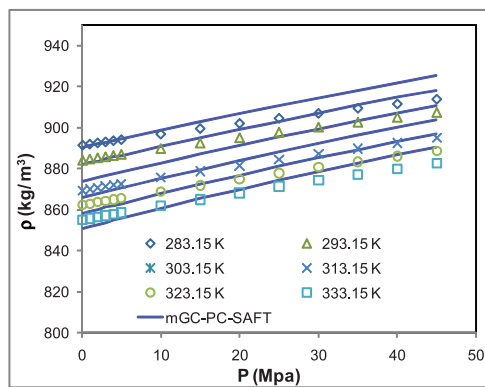
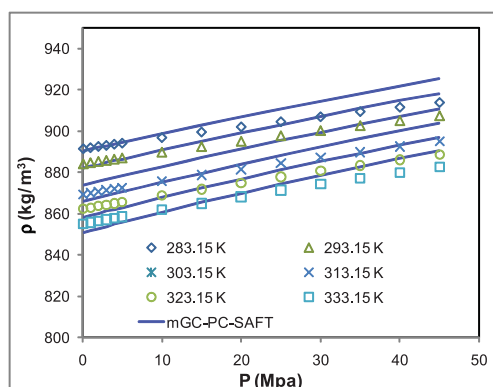


**Fig.10.** Density isotherms for soybean + rapeseed biodiesel (left) and rapeseed + palm biodiesel (right). The symbols represent the experimental data, while the continuous curves correspond to the mGC-PC-SAFT prediction. Data taken from ref. [44]

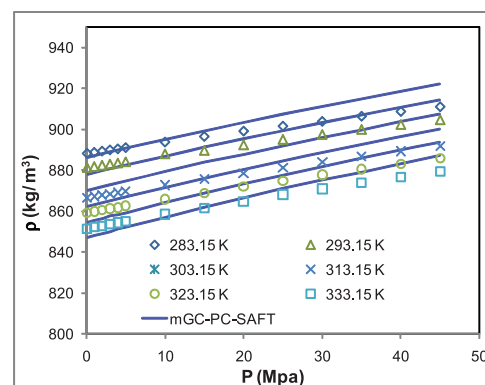
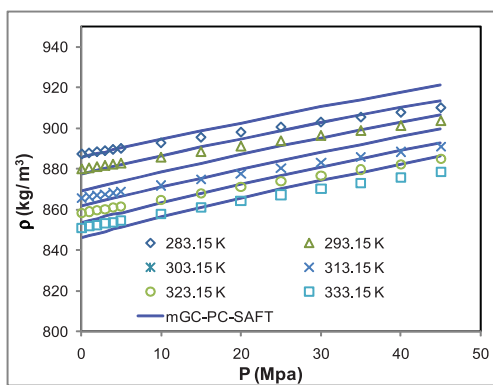


**Fig.11.** Density isotherms for soybean + palm biodiesel (left) and soybean + rapeseed + palm biodiesel (right). The symbols represent the experimental data, while the continuous curves correspond to the mGC-PC-SAFT prediction. Data taken from ref. [44]

## Conclusions

PpT at atmospheric pressure and very high pressure of 10 biodiesel mixtures were predicted with mGC-PC-SAFT. Along with chemical group parameters determined from the PVT data of 10 first components of the alkyl-esters series, PpT densities were used to predict biodiesel densities based on information of their FAME compositions. It was shown that mGC-PC-SAFT is able to predict the liquid density of both pure heavy alkyl-esters and biodiesel with less than 2% deviation in general. In particular, mGC-PC-SAFT provides an uncertainty that is close to the experimental uncertainties of the experimental data and can thus be an interesting tool for the design of biofuels.

Two different modeling approaches were used to compare the prediction performance: the CPA EoS and mGC-PC-SAFT developed in this work. The first method presented an AAD slightly more important than that obtained with mGC-PC-SAFT, the modified GC combined with the PC-SAFT EoS was shown to predict biodiesel temperature and pressure dependent density with an OAAD of 1% while also providing information concerning the phase equilibria of the biodiesel systems. These results clearly showed that, provided that the biodiesel FAME composition is known, the predictive methods investigated here can be used to predict liquid density of biodiesel fuels in a wide range of temperatures and pressures.

## References

1. D.Y.C.Leung, X.Wu and M.K.H.Leung. *A review on biodiesel production using catalyzed transesterification*. Applied Energy. 2010; 87(4): p. 1083 - 1095.
2. L.T.Thanh, K.Okitsu, L.V.Boi and Y.Maeda. *Catalytic technologies for biodiesel fuel production and utilization of glycerol a review*. Catalysts. 2012; 2(1): p. 191 - 222.
3. A.Ramadhass, S.Jayaraj and C.Muraleedharan. *Use of vegetable oils as IC engine fuels a review*. Renewable Energy. 2004; 29(5): p. 727 - 742.
4. S.Jaichandar and K.Annamalai. *The status of biodiesel as an alternative fuel for diesel engine an overview*. Journal of Sustainable Energy & Environment. 2011; 2: p. 71 - 75.
5. Y.C.Su, Y.A.Liu, C.A.Diaz Tovar and R.Gani. *Selection of prediction methods for thermophysical properties for process modeling and product design of biodiesel manufacturing*. Industrial & Engineering Chemistry Research. 2011; 50(11): p. 6809 - 6836.
6. L.F.Gutiérrez, Ó.J.Sánchez and C.A.Cardona. *Process integration possibilities for biodiesel production from palm oil using ethanol obtained from lignocellulosic residues of oil palm industry*. Bioresource Technology. 2009; 100(3): p. 1227 - 1237.
7. F.I.Gomez-Castro, V.Rico-Ramirez, J.G.Segovia-Hernandez and S.Hernandez. *Feasibility study of a thermally coupled reactive distillation process for biodiesel production*. Chemical Engineering and Processing: Process Intensification. 2010; 49(3): p. 262 - 269.
8. A.Apostolakou, I.Kookos, C.Marazioti and K.Angelopoulos. *Techno-economic analysis of a biodiesel production process from vegetable oils*. Fuel Processing Technology. 2009; 90(7): p. 1023 - 1031.
9. British Standards Institution (BSI). *BS EN 14214 automotive fuels - Fatty acid methyl esters (FAME) for diesel engines - requirements and test methods*. BSI: London, U.K. 2009.
10. American society for testing and materials (ASTM). *ASTM D6751-09. Standard specification for biodiesel fuel blend stock (B100) for middle distillate fuels*. ASTM: West Conshohocken, PA, 2009.
11. *Nhiên liệu diesel sinh học gốc (B100)*. Yêu cầu kỹ thuật (Biodiesel fuel blend stock (B100) TCVN 7717:2007. 2007; (2718/QĐ-BKHCHN): p. 1 - 16.
12. R.Payri, F.Salvador, J.Gimeno and G.Bracho. *The effect of temperature and pressure on thermodynamic properties of diesel and biodiesel fuels*. Fuel. 2011; 90(3): p. 1172 - 1180.
13. D.Tziourtzioumis and A.Stamatelos. *Effects of a 70% biodiesel blend on the fuel injection system operation during steady-state and transient performance of a common rail diesel engine*. Energy Conversion and Management. 2012.
14. F.Boudy and P.Seers. *Impact of physical properties of biodiesel on the injection process in a common-rail direct injection system*. Energy Conversion and Management. 2009; 50(12): p. 2905 - 2912.
15. H.Veny, S.Baroutian, M.K.Aroua, M.Hasan, A.A.Raman and N.M.N.Sulaiman. *Density of Jatropha curcas seed oil and its methyl esters: measurement and*

estimations. *International Journal of Thermophysics*. 2009; 30(2): p. 529 - 541.

16. M.Dzida and P.Prusakiewicz. *The effect of temperature and pressure on the physicochemical properties of petroleum diesel oil and biodiesel fuel*. *Fuel*. 2008; 87(10 - 11): p. 1941 - 1948.

17. M.M.Budeanu, S.Radu and V.Dumitrescu. *Comparing some models for predicting the density of liquid mixtures*. *Rev. Chim.* 2010; 61: p. 322 - 328.

18. K.Anand, A.Ranjan and P.S.Mehta. *Predicting the density of straight and processed vegetable oils from fatty acid composition*. *Energy & Fuels*. 2010; 24(5): p. 3262 - 3266.

19. F.X.Feitosa, M.L.Rodrigues, C.B.Veloso, Jr.C.L., Cavalcante, M.C.G.Albuquerque and H.B.De Sant'Ana. *Viscosities and densities of binary mixtures of coconut + colza and coconut + soybean biodiesel at various temperatures*. *Journal of Chemical & Engineering Data*. 2010; 55(9): p. 3909 - 3914.

20. M.Tat and J.Van Gerpen. *The specific gravity of biodiesel and its blends with diesel fuel*. *Journal of the American Oil Chemists' Society*. 2000; 77(2): p. 115 - 119.

21. E.Benmekki and G.Mansoori. *Pseudoization technique and heavy fraction characterization with equation of state models*. *Advance in Thermodynamics*. 1989; 1: p. 57 - 78.

22. H.S.Elbro, A. Fredenslund and P.Rasmussen. *Group contribution method for the prediction of liquid densities as a function of temperature for solvents, oligomers, and polymers*. *Ind. Eng. Chem. Res.* 1991; 30(12): p. 2576 - 2582.

23. M.J.Pratas, S.Freitas, M.B.Oliveira, S.I.C.Monteiro, A.I.S.Lima and J.O.A.P.Coutinho. *Densities and Viscosities of minority fatty acid methyl and ethyl esters present in biodiesel*. *Journal of Chemical & Engineering Data*. 2011; 56(5): p. 2175 - 2180.

24. J. Gross and G.Sadowski. *Perturbed-Chain SAFT: An equation of state based on a perturbation theory for chain molecules*. *Ind. Eng. Chem. Res.* 2001; 40: p. 1244 - 1260.

25. J. Gross and G.Sadowski. *Application of perturbation theory to a hard-chain reference fluid: an equation of state for square-well chains*. *Fluid Phase Equilibria*. 2000; 168: p. 183 - 199.

26. J.C.De Hemptinne, R.Lugo, Nguyen Huynh Dong and A.Barreau. *Predictive models and their need in the biofuel industry*. VIII Iberoamerican Conference on Phase equilibria and fluid properties for process design - equifase 2009, Algarve - Praia da Rocha, Portugal, Invited oral presentation. 17 - 21 October 2009.

27. Nguyen Huynh Dong, J.P.Passarello, P.Tobaly and J.C.De Hemptinne. *GC-SAFT as a predictive tool for computing VLE and LLE of systems involved in oil and gas industry*. *Proceedings of the 23<sup>rd</sup> European Symposium on Applied Thermodynamics - 2008 (ESAT)*, Cannes, France, Oral presentation. 2008.

28. Nguyen Huynh Dong, M.Benamira, J.P.Passarello, P. Tobaly, and J.C.De Hemptinne. *Application of GC-SAFT EOS to polycyclic aromatic hydrocarbons*. *Fluid Phase Equilibria*. 2007; 254: p. 60 - 66.

29. J.Gross and J.Vrabec. *An Equation-of-State contribution for Polar Components: Dipolar Molecules* *AIChE Journal*. 2006; 52(3): p. 1194 - 1204.

30. P.K.Jog and W.G.Chapman. *Application of Wertheim's thermodynamic perturbation theory to dipolar hard sphere chains*. *Molecular Physics*, 1999. 97(3): p. 307 - 319.

31. C.G.Gray, and K.E. Gubbins. *Theory of molecular fluids*. New York: Oxford University Press. 1984.

32. Nguyen Huynh Dong, J.P.Passarello, P.Tobaly and J.C.De Hemptinne. *Application of GC-SAFT EOS to polar systems using a segment approach* *Fluid Phase Equilibria*. 2008; 264: p. 62 - 75.

33. C.H.Twu and K.E.Gubbins. *Thermodynamics of polyatomic fluid mixtures-II: Polar, quadrupolar and octopolar molecules*. *Chemical Engineering Science*. 1978; 33(7): p. 879 - 887.

34. S.G.Sauer and W.G. Chapman. *A parametric study of dipolar chain theory with applications to ketone mixtures*. *Ind. Eng. Chem. Res.* 2003; 42: p. 5687 - 5696.

35. M.Mourah, Nguyen Huynh Dong, J.P.Passarello, J.C.De Hemptinne and P.Tobaly. *Modeling LLE & VLE of methanol + n-alkane series using GC-PC-SAFT with a group contribution kij*. *Fluid Phase Equilibria*, 2010. 298: p. 154 - 168.

36. A.Dominik, W.G.Chapman, M.Kleiner and G.Sadowski. *Modeling of polar systems with the perturbed-chain SAFT equation of state. Investigation of the*

performance of two polar terms. *Ind. Eng. Chem. Res.* 2005; 44: p. 6928 - 6938.

37. N.M.Al-Saifi, E.Z.Hamad and P.Englezos. *Prediction of vapor-liquid equilibrium in water-alcohol-hydrocarbon systems with the dipolar perturbed-chain SAFT equation of state* *Fluid Phase Equilibria*. 2008; 271(1 - 2): p. 82 - 93.

38. S.Tamouza, J.P.Passarello, P.Tobaly and J.C.De Hemptinne. *Group contribution method with SAFT EOS applied to vapor liquid equilibria of various hydrocarbon series*. *Fluid Phase Equilibria* 2004. 222 - 223: p. 67 - 76.

39. Nguyen Huynh Dong et al. *Ind. Eng. Chem. Res.* In preparation. 2012.

40. Nguyen Huynh Dong, A.Falaix, J.P.Passarello, P.Tobaly and J.C.De Hemptinne. *Predicting VLE of heavy esters and their mixtures using GC-SAFT*. *Fluid Phase Equilibria*. 2008; 264: p. 184 - 200.

41. S.P.Singh and D.Singh. *Biodiesel production through the use of different sources and characterization of oils and their esters as the substitute of diesel: A review*. *Renewable and Sustainable Energy Reviews*. 2010; 14(1): p. 200 - 216.

42. Nguyen Thi Thanh Xuan, S.Tamouza, P.Tobaly, J.P.Passarello and J.C.De Hemptinne. *Application of group contribution SAFT equation of state (GC-SAFT) to model phase behaviour of light and heavy esters*. *Fluid Phase Equilibria*. 2005; 238: p. 254 - 267.

43. A.Tihic, G.M.Kontogeorgis, N.Von Solms, M.L.Michelsen, and L.Constantinou. *A predictive Group-Contribution simplified PC-SAFT equation of state: Application to polymer systems*. *Ind. Eng. Chem. Res.* 2008.

44. M.J.Pratas, M.B.Oliveira, M.J.Pastoriza-Gallego, A.J.Queimada, and J.A.P.Coutinho. *High-Pressure biodiesel density: Experimental measurements, correlation, and Cubic-Plus-Association equation of state (CPA EoS) modeling*. *Energy & Fuels*. 2011; 25: p. 3806 - 3814.

45. T.A.Scott, D.Macmillan, and E.H.Melvin. *Vapor pressures and distillation of methyl esters of some fatty acids*. *Industrial & Engineering Chemistry*. 1952; 44(1): p. 172 - 175.

46. A. Rose and W.R. Supina. *Vapor pressure and vapor-liquid equilibrium data for methyl esters of the common saturated normal fatty acids*. *Journal of Chemical & Engineering Data*. 1961. 6(2): p. 173 - 179.

47. A.C.G.Van Genderen, J.C.Van Miltenburg, J.G.Blok, M.J.Van Bommel, P.J.Van Ekeren, G.J.K.Van Den

Berg, and H.A.J.Oonk. *Liquid-vapour equilibria of the methyl esters of alkanolic acids: vapour pressures as a function of temperature and standard thermodynamic function changes*. *Fluid Phase Equilibria*. 2002; 202: p. 109 - 120.

48. M.J.Pratas, S.Freitas, M.B.Oliveira, S.C.Monteiro, A.S.Lima, and J.A.P.Coutinho. *Densities and viscosities of fatty acid methyl and ethyl esters*. *J. Chem. Eng. Data*. 2010; 55: p. 3983 - 3990.

49. M.J.Pratas, S.V.D.Freitas, M.B.Oliveira, S.I.C.Monteiro, A.I.S.Lima, and J.O.A.P.Coutinho. *Biodiesel density: experimental measurements and prediction models*. *Energy & Fuels*. 2011; 25(5): p. 2333 - 2340.

50. DIPPR, Design Institute for Physical Property Data, Thermophysical Properties Database. 2002.

51. L.F.Ramírez-Verduzco, B.E.García-Flores, J.E.Rodríguez-Rodríguez, and A.Del Rayo Jaramillo-Jacob. *Prediction of the density and viscosity in biodiesel blends at various temperatures*. *Fuel*. 2011; 90(5): p. 1751-1761.

52. S.Baroutian, M.K.Aroua, A.A.A.Raman, and N.M.N.Sulaiman. *Density of palm oil-based methyl ester*. *Journal of Chemical & Engineering Data*. 2008; 53(3): p. 877 - 880.

53. M.L.Huber, E.W.Lemmon, A.Kazakov, L.S.Ott, and T.J.Bruno. *Model for the thermodynamic properties of a biodiesel fuel*. *Energy & Fuels*. 2009; 23(7): p. 3790 - 3797.

54. P.Benjumea, J.Agudelo, and A.Agudelo. *Basic properties of palm oil biodiesel-diesel blends*. *Fuel*. 2008; 87(10 - 11): p. 2069 - 2075.

55. W.A.Burgess, D.Tapriyal, B.D.Morreale, Y.Wu, M.A.McHugh, H.Baled, and R.M.Enick. *Prediction of fluid density at extreme conditions using the perturbed-chain SAFT equation correlated to high temperature, high pressure density data*. *Fluid Phase Equilibria*. 2012; 319: p. 55 - 66.

56. Nguyen Huynh Dong, J.P.Passarello, P.Tobaly, and J.C.De Hemptinne. *Modeling phase equilibria of asymmetric mixtures using a group contribution SAFT (GC-SAFT) with a kij correlation method based on London's theory. Part 1: application to CO<sub>2</sub> + n-alkane, methane + n-alkane and ethane + n-alkane systems*. *Ind. Eng. Chem. Res.* 2008; 47(22): p. 8847 - 8858.